

Annual cycle of air-sea CO₂ exchange in an Arctic Polynya Region

B. G. T. Else,¹ T. N. Papakyriakou,¹ M. G. Asplin,¹ D. G. Barber,¹ R. J. Galley,¹ L. A. Miller,² and A. Mucci³

Received 12 June 2012; revised 6 December 2012; accepted 20 December 2012; published 9 May 2013.

[1] During the Canadian International Polar Year projects in the Cape Bathurst polynya region, we measured a near-complete annual cycle of sea surface CO₂ ($p\text{CO}_{2\text{sw}}$), atmospheric CO₂ ($p\text{CO}_{2\text{atm}}$), sea surface temperature (SST), salinity (S), and wind speed (U). In this paper, we combine these data with ancillary measurements of sea ice concentration (C_i) to estimate the mean annual (September 2007–September 2008) air–sea CO₂ exchange for the region. For the non-freezing seasons the exchange was calculated using a standard bulk aerodynamic approach, whereas during the freezing seasons we extrapolated eddy covariance measurements of CO₂ exchange. Our results show that in 2007–08 the region served as a net sink of atmospheric CO₂ at a mean rate of $-10.1 \pm 6.5 \text{ mmol m}^{-2} \text{ d}^{-1}$. The strongest calculated uptake rate occurred in the fall when wind velocities were highest, $p\text{CO}_{2\text{sw}}$ was significantly lower than $p\text{CO}_{2\text{atm}}$, and ice was beginning to form. Atmospheric CO₂ uptake was calculated to occur (at lower rates) throughout the rest of the year, except for a brief period of outgassing during late July. Using archival U , C_i , and $p\text{CO}_{2\text{sw}}$ data for the region, we found that winds in 2007–08 were 25–35 % stronger than the decadal mean and were predominately easterly, which appears to have induced a relatively late freeze-up (by ~ 3 weeks relative to mean conditions) and an early polynya opening (by ~ 4 weeks). In turn, these conditions may have given rise to a higher CO₂ uptake than normal. Estimated winter CO₂ exchange through leads and small polynya openings made up more than 50% of the total CO₂ uptake, consistent with recent observations of enhanced CO₂ exchange associated with open water components of the winter icescape. Our calculations for the Cape Bathurst polynya region are consistent with past studies that estimated the total winter CO₂ uptake in Arctic coastal polynyas to be on the order of $10^{12} \text{ g C yr}^{-1}$.

Citation: Else, B. G. T., T. N. Papakyriakou, M. G. Asplin, D. G. Barber, R. J. Galley, L. A. Miller, and A. Mucci (2013), Annual cycle of air-sea CO₂ exchange in an Arctic 1 Polynya region, *Global Biogeochem. Cycles*, 27, 388–398, doi:10.1002/gbc.20016.

1. Introduction

[2] Polynyas (areas of recurring open water that exist when a complete ice cover would be expected) are wide spread across the Arctic and Antarctic but only account for a small portion of the total area of polar seas [Barber and Massom, 2007]. Despite their limited extent, at times they provide the only direct connection between the atmosphere and the

underlying ocean, making them important sites for air–sea interactions. The air–sea exchange of CO₂ during time periods when polynyas occur has received considerable interest (e.g. Miller and DiTullio [2007]), but significant exchange has also been observed during other seasons [Else et al., 2011]. By tracking air–sea CO₂ transfer through an entire annual cycle in geographic areas that host polynyas (areas we term “polynya regions”) we can better quantify their contribution to global and regional atmospheric carbon budgets.

[3] The potential for CO₂ exchange at the air–sea interface is determined by the CO₂ gradient across the interface, $\Delta p\text{CO}_2 = p\text{CO}_{2\text{sw}} - p\text{CO}_{2\text{atm}}$, where $p\text{CO}_{2\text{sw}}$ and $p\text{CO}_{2\text{atm}}$ are the sea surface and atmospheric partial pressures of CO₂, respectively. To date, almost all observations of $\Delta p\text{CO}_2$ in polynya regions have been made in spring, summer, and fall, forcing annual budgets of CO₂ exchange to rely on assumptions about the winter season. For instance, in the Northeast Water (NEW) polynya, Yager et al. [1995] observed low mid-summer $p\text{CO}_{2\text{sw}}$ caused by strong primary production earlier in the spring. They hypothesized that the region acted

Additional supporting information may be found in the online version of this article.

¹Centre for Earth Observation Science, Department of Environment and Geography, University of Manitoba, Winnipeg, Manitoba, Canada.

²Institute of Ocean Sciences, Fisheries and Oceans Canada, Sidney, British Columbia, Canada.

³GEOTOP, Department of Earth and Planetary Science, McGill University, Montreal, Québec, Canada.

Corresponding author: B.G.T. Else, Centre for Earth Observation Science, Department of Environment and Geography, University of Manitoba, Winnipeg, Manitoba, Canada. (b_else@umanitoba.ca)

©2013. American Geophysical Union. All Rights Reserved
0886-6236/13/10.1002/gbc.20016

as a CO₂ sink during the open water season with strong fall winds exploiting the negative $\Delta p\text{CO}_2$ gradient. They also predicted that $\Delta p\text{CO}_2$ would become positive in winter due to excess respiration, but that the winter ice cover would prevent any outgassing. Support for this hypothesized cycle was provided by *Miller et al.* [2002] who observed a brief positive $\Delta p\text{CO}_2$ before the spring opening of the Northwater polynya, followed by strongly negative $\Delta p\text{CO}_2$ as the ice cleared. Likewise, modelling [*Sweeney, 2003*] and summer $p\text{CO}_{2,\text{sw}}$ measurements [*Sweeney et al., 2000*] in the Ross Sea polynya regions (Antarctica) have revealed a similar cycle (see also the review by *Miller and DiTullio* [2007]).

[4] Although the cycle described in *Yager et al.* [1995] has played an important role in shaping our understandings of air–sea CO₂ exchange in seasonal sea ice areas, recent observations have revealed some important deviations. In winter, ice remains mobile in many of these regions, allowing the formation of open-water leads and winter polynyas. If such regions follow the $p\text{CO}_{2,\text{sw}}$ cycles described above, winter outgassing should occur wherever open water is found, possibly at a rate that would balance the summer/fall uptake. Instead, *Anderson et al.* [2004] reported water column measurements of dissolved inorganic carbon (DIC) and chlorofluorocarbons from the Storfjorden polynya (Svalbard, Norway) indicating a strong winter uptake of atmospheric CO₂. Using similar data, *Omar et al.* [2005] calculated the rate of winter CO₂ uptake in that region to be about 10 times larger than the surrounding non–polynya areas. In the Cape Bathurst polynya region (southeastern Beaufort Sea, Canada), we recently observed episodes of strong winter uptake using micrometeorological techniques (i.e., eddy covariance) [*Else et al., 2011*], and we were able to show that $\Delta p\text{CO}_2$ remained negative through the entire winter [*Else et al. 2012a*].

[5] In this paper, we use the $p\text{CO}_{2,\text{sw}}$ data set described in *Else et al.* [2012a], combined with our direct observations of winter fluxes [*Else et al. 2011*] to calculate a full–year (2007–08) air–sea CO₂ flux budget for the Cape Bathurst polynya region. In doing so, we create one of the most complete estimates of annual air–sea CO₂ exchange available for any polar sea, allowing greater insight into the role of polynya regions in atmospheric carbon cycling. Our approach updates a preliminary estimate of CO₂ exchange created for the region by *Shadwick et al.* [2011]. Finally, we examine whether the conditions experienced in 2007–08 (ice, ocean, atmosphere) represent a “typical” annual cycle for this region, and we discuss the implications of our results at the circumpolar scale.

2. Methods

2.1. Data Sources

[6] The majority of the data required for this study were collected during the International Polar Year ArcticNet and Circumpolar Flaw Lead System Study projects. The projects were conducted onboard the research icebreaker CCGS *Amundsen*, and are summarized in *ArcticNet Inc.* [2010] and *Barber et al.* [2010]. Multidisciplinary sampling was carried out during both projects while the ship remained mobile in the Cape Bathurst polynya region for most of an annual cycle (Figure 1). In this paper, we used data that were collected from October 22, 2007 to August 2, 2008 in

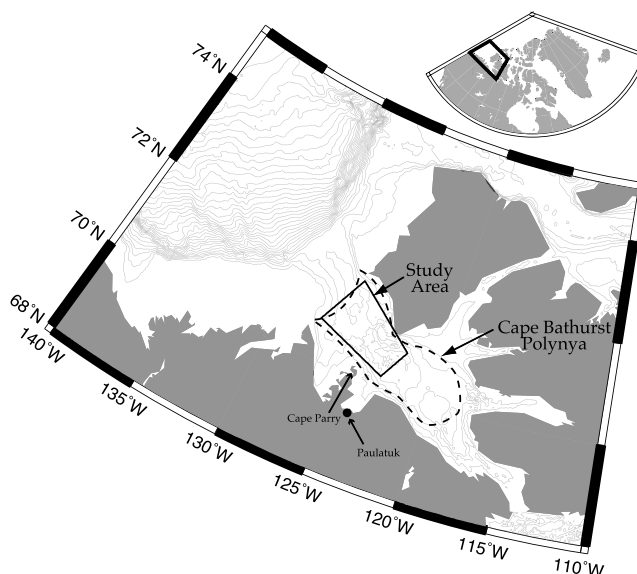


Figure 1. The study area. The dashed line outlines the approximate location of the Cape Bathurst polynya (and also outlines Amundsen Gulf). The solid polygon denotes the area in which field data were collected.

western Amundsen Gulf, the primary location of ship activities (Figure 1). To create CO₂ flux estimates spanning a complete annual cycle, we defined a study period of September 15, 2007 to September 14, 2008, necessitating an extension of the data by ~ 6 weeks on either side of the field program. Various ancillary data sets were required to facilitate this extension, and fill other gaps in the field data.

[7] **Wind speed** was measured by a propeller anemometer installed on an open–lattice meteorological tower located at the bow of the research vessel (see *Else et al.* [2011] for instrument details, including data quality control). We used hourly averages, and when ship based data were not available (usually due to ship orientation) we used hourly data collected at the Cape Parry (preferably) or the Paulatuk Environment Canada weather stations (see Figure 1). All wind speed data were scaled to a height of 10 m above sea level, and the different data sources showed reasonable agreement when compared during periods of overlap (root mean square differences of velocity on the order of $4\text{--}5\text{ m s}^{-1}$).

[8] **Ice concentration** was obtained at daily intervals from the University of Bremen AMSR-E passive microwave satellite imagery products [*Spreen et al., 2008*]. This data product reports ice concentration on a ratio scale from 0 (ice free) to 1 (complete ice cover) at a spatial resolution of 6.25 km.

[9] **Sea surface temperature (SST)** was measured during the field experiment using a ship–based CTD (SeaBird 911+). The CTD was deployed over the side of the ship during the open water seasons, providing SST samples at a water depth of ~ 2 m. During the winter the CTD was deployed through a moon pool, and the SST sampling depth was ~ 10 m (as per *Else et al.* [2012a], the error associated with these different depth measurements is small). To extend the SST data set beyond the duration of the field program, we used daily L3 MODIS-Aqua daytime $11\ \mu$ SST satellite imagery.

[10] **Salinity** was also measured using the ship–based CTD. No supplemental measurements were available beyond the

dates of the sampling program, so we used a simple interpolation based on a polynomial fit to the field data.

[11] $p\text{CO}_{2\text{atm}}$ was measured on the meteorological tower at the bow of the ship, using a near-infrared gas analyzer (LiCor model LI-7000) system which drew sample air from an inlet located ~ 14 m above sea level. The instrument was calibrated regularly [Else *et al.*, 2011; Else *et al.*, 2012b], and data acquired when the sample air may have been contaminated by ship emissions were removed in post-processing. For the time period when the ship was not in the area, we used data from the Scripps CO₂ Program sampling station at Barrow, Alaska (approximately 1000 km west of our study area) [Keeling *et al.*, 2001]. Those data were available approximately bi-weekly during the winter and weekly through the rest of the year, and showed good agreement with our ship-based samples (root mean square error 4.1 ppm, based on 14 dates when coincident measurements were made at Barrow and on the CCGS *Amundsen*).

[12] $p\text{CO}_{2\text{sw}}$ was measured using a shower-type equilibrator connected to a short (~ 5 m) intake line with an inlet at ~ 5 m depth. The equilibrator's headspace air was continuously cycled through an infrared gas analyzer (LI-7000) calibrated daily with ultra-pure nitrogen (to set the instrument's zero reading) and a CO₂-air mixture traceable to WMO standards (to set the span reading). A detailed description of this instrument, its components, and the reproducibility of the measurements can be found in Else *et al.* [2012a] and Else *et al.* [2012b]. To extend these data beyond the field study time period, we assumed that changes in $p\text{CO}_{2\text{sw}}$ between August and October are modulated by water temperature. We used measurements of $p\text{CO}_{2\text{sw}}$ and SST from the start of the field season to define an initial state, and then calculated $p\text{CO}_{2\text{sw}}$ for the 6 weeks prior to sampling using the thermodynamic equations of Takahashi *et al.* [1993] and the MODIS SST data. We did likewise for the 6 weeks after the end of the field sampling program. This is of course a simplification, but the results of this approach (shown in Figure 2c & e, discussed below) yield a reconstruction very similar to what might be achieved by simple interpolation between summer 2008 and fall 2007 data (i.e., the approach used by Shadwick *et al.* [2011]).

2.2. Flux Calculation

[13] For any ice-affected sea it is useful to partition the net surface CO₂ flux ($F_{\text{CO}_{2\text{total}}}$) into a component that describes the exchange between open seawater and the atmosphere (which we denote $F_{\text{CO}_{2\text{as}}}$) and one that describes exchange between the ice surface and the atmosphere ($F_{\text{CO}_{2\text{ai}}}$):

$$F_{\text{CO}_{2\text{total}}} = F_{\text{CO}_{2\text{as}}} + F_{\text{CO}_{2\text{ai}}} \quad (1)$$

[14] Although not often considered, observations of significant $F_{\text{CO}_{2\text{ai}}}$ have been reported using micrometeorological techniques [Semiletov *et al.*, 2004; Zemmelen *et al.*, 2006; Miller *et al.*, 2011; Papakyriakou and Miller, 2011], chamber techniques [Semiletov *et al.*, 2004; Nomura *et al.*, 2010; Geilfus *et al.*, 2012], and laboratory experiments [Nomura *et al.*, 2006]. While the community is approaching consensus on the expected direction of these exchanges (CO₂ outgassing during winter, CO₂ uptake in the spring/summer), the observed fluxes vary by 1–2 orders of

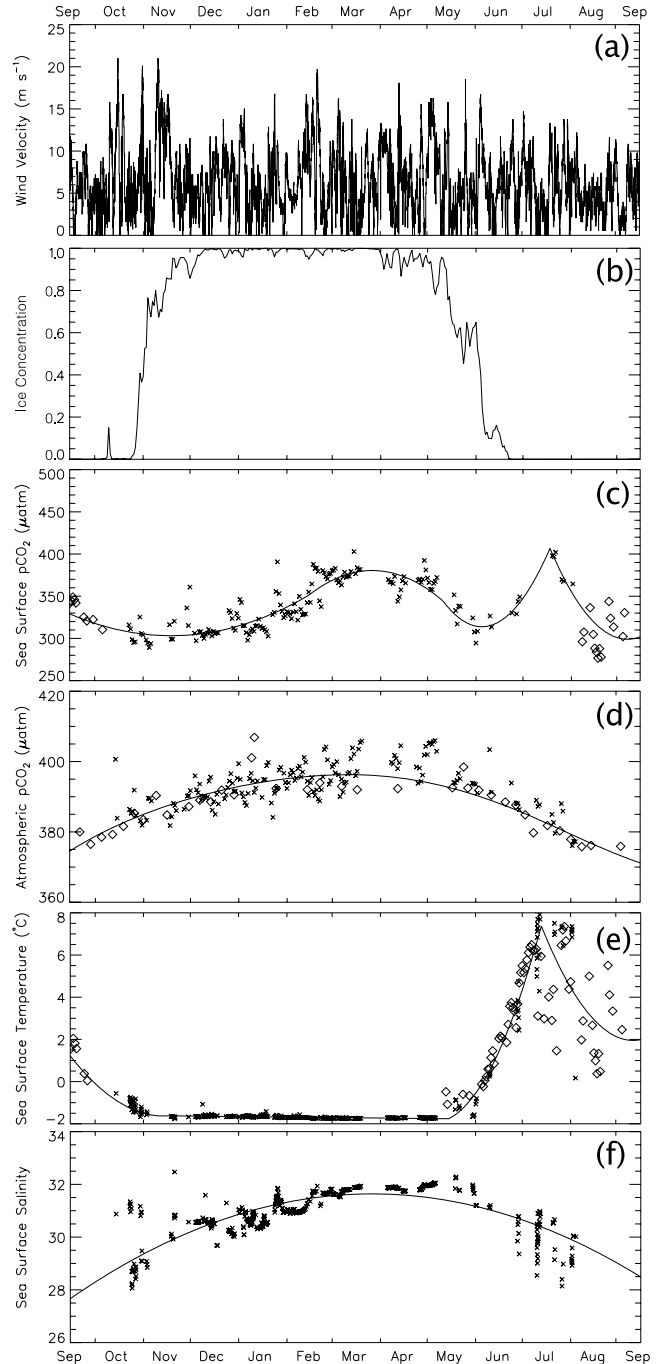


Figure 2. Observations of (a) wind speed, (b) ice concentration, (c) $p\text{CO}_{2\text{sw}}$ (x symbols are observed daily means, open diamonds are extrapolated data as per section 2.1), (d) $p\text{CO}_{2\text{atm}}$ (x symbols were observed on the research vessel, open diamonds are from Barrow, Alaska), (e) sea surface temperature (x symbols were observed on the research vessel, open diamonds were obtained from the MODIS instrument), and (f) salinity (measured onboard the research vessel). For panels b-f, the solid lines are the fitted polynomials that were used for resampling the data to one-hour intervals.

magnitude. Therefore, in this paper we limit ourselves to deriving only $F_{\text{CO}_{2\text{as}}}$, with the understanding that $F_{\text{CO}_{2\text{ai}}}$ could be added to create a more complete budget as the state of the science evolves.

[15] To calculate $F_{CO_{2as}}$, we used a standard form of the bulk flux equation, scaled by the ice concentration (C_i , reported as a fraction of the areal coverage):

$$F_{CO_{2as}} = k\alpha\Delta pCO_2(1 - C_i) \quad (2)$$

where k is the gas transfer velocity, and α is the solubility of CO₂ in seawater (a function of SST and salinity). During the non-freezing season (i.e., when air temperature exceeds SST), we used the parameterization of *Sweeney et al.* [2007] to calculate k :

$$k = 0.27U^2(Sc/660)^{(-1/2)} \quad (3)$$

where U is the wind speed at 10 m height, and Sc is the Schmidt number (a function of SST). The time period that we applied this k parameterization to was September 15 – November 14, 2007 and May 16 – September 14, 2008 (see below for explanation), and we denote those fluxes as $F_{CO_{2asnorm}}$.

[16] It is important to note that this approach makes the implicit assumption that the *Sweeney et al.* [2007] k - U relationship (derived for the open ocean) is applicable for the conditions encountered during this time period. However, when sea ice is present there is evidence to suggest that modification of surface water turbulence (and hence k) may occur [*Loose and Schlosser*, 2011]. This modification may be due in part to fetch limitations imposed on open water patches by the surrounding sea ice. At low wind speeds, short fetches create steep waves [*Vickers and Mahrt*, 1997] which are linked to higher gas transfer [*Zappa et al.*, 2004], but at higher wind speed, whitecap formation and bubble-mediated gas exchange becomes restricted [*Woolf*, 2005]. Furthermore, sea ice itself can generate turbulence via convection and current shear [*McPhee*, 2005], but it also may attenuate wind-driven turbulence by reflection and scattering of wind waves [*Masson and LeBlond*, 1989]. Fortunately, the spatio-temporal extents of conditions where these interactions are most severe tends to be limited – for example, in the Cape Bathurst polynya the spring break-up and fall freeze-up periods (when C_i is most variable) only last 7 and 3 weeks (respectively) on average [*Galley et al.*, 2008]. Therefore, open ocean k - U parameterizations have been widely used in Arctic seas (e.g. *Bates and Mathis* [2009] and references therein), with the understanding that calculated fluxes await future refinement.

[17] Of more relevance to our study is the fact that standard k - U parameterizations cannot account for observations of enhanced winter fluxes (e.g. *Anderson et al.* [2004]; *Loose et al.* [2009]; *Else et al.* [2011]). These enhanced fluxes (which we denote as $F_{CO_{2as:enh}}$) appear to be associated with the formation of new sea ice in open water [*Else et al.*, 2011], which in the Cape Bathurst polynya region typically occurs in flaw leads throughout the entire winter. To provide a rough estimate of how strong this enhanced winter flux might be, we calculated the mean winter transfer velocity from measurements made in the Cape Bathurst polynya ($\bar{k}_{enh} = 458 \pm 334$ cm hr⁻¹, [*Else et al.*, 2011]) and used that value in equation 2. The \bar{k}_{enh} value was derived from 32 half-hour eddy covariance samples, which span a large range of mean wind speed (4 – 18 m s⁻¹), air temperature (-5 – -23 °C), sensible heat flux (-15 – 150 W m⁻²) and ΔpCO_2 (-80 – -38 μ atm) conditions. For this study, we calculated $F_{CO_{2as:enh}}$ from

November 15 2007 – May 15 2008, which corresponds to the time period when SST was at the freezing point (see section 3.1), surface air temperatures were consistently lower than SST, and conditions were typically within the bounds of those experienced when collecting the k_{enh} data.

[18] It is worth noting that we did find significant non-linear relationships between observations of k_{enh} and wind speed ($\ln(k_{enh}) = 0.16U + 3.97$, $r^2 = 0.55$) and k_{enh} and air temperature ($\ln(k_{enh}) = -0.09 T_{air} + 4.49$, $r^2 = 0.33$). Both of these relationships are consistent with our hypothesis that the flux enhancement is partly driven by wind and high sensible heat fluxes that produce a very turbulent sea surface [*Else et al.*, 2011]. However, we decided that it was imprudent to use parameterizations based on these variables at this time given how limited the data set is, and given that causal links between these variables and k_{enh} have not yet been proven. Instead, using the mean k_{enh} value (and incorporating the considerable variability around that mean) gives us a first-order estimate of how strong the flux may have been through the winter.

2.3. Data Integration

[19] A key challenge for the flux calculations was the discontinuous sampling intervals inherent in some of the variables. The field data set (SST, salinity, pCO_{2sw} , pCO_{2atm}) was discontinuous because the ship would often leave the study area for several days to sample in other locations. The Scripps CO₂ data sampling interval was also discontinuous (sampling occurred weekly through most of the year, and was less frequent during the winter), and SST was only retrievable from MODIS imagery on cloud-free days. On the other hand, the wind speed and AMSR-E ice concentration data were acquired continuously at regular intervals. To deal with this issue, we fit polynomials to the pCO_{2sw} , pCO_{2atm} , SST, and salinity data to interpolate over periods of missing data. This approach gives a generalized view of the annual cycle of these variables and eliminates high-frequency (e.g. diurnal) variability, which has been observed to play an important role in CO₂ exchange at low latitudes (e.g. *McGillis et al.* [2004]). However, we did not observe significant high-frequency variability in pCO_{2sw} in this region [*Else et al.*, 2012a], and we do not expect high-frequency variability in pCO_{2atm} , SST, or salinity to play a strong role in influencing CO₂ flux calculations. The variability that did occur in these parameters was characterized by calculating standard deviations around the polynomial fits, and the standard deviations were used in error evaluation of the resulting CO₂ flux calculations.

3. Results

3.1. Observed Conditions

[20] Time series of the variables required for the flux calculations are shown in Figure 2. Wind velocities (Figure 2a) were highest between October and November 2007, with a mean speed (and standard deviation) of 7.2 ± 4.8 m s⁻¹ and storm episodes with sustained winds in excess of 15 m s⁻¹. Over the winter (December to March) winds were somewhat weaker, with mean velocities of 6.2 ± 3.7 m s⁻¹ and storms that rarely sustained winds in excess of 15 m s⁻¹. Spring (April to June) saw a slight increase in mean winds (6.5 ± 4.0 m s⁻¹) and similar storm activity. Winds were weakest through the open water season (July to September 2008) with mean velocities of 5.4 ± 3.0 m s⁻¹ and limited storm activity.

[21] The time series of C_i is shown in Figure 2b, and an animation showing C_i over the annual cycle is available in supplemental Figure S1. Ice began forming in the region around October 25, and reached 0.99 on December 10. Throughout the winter season the ice cover remained mobile, resulting in leads and small polynyas that kept C_i fluctuating between 0.95 and 0.99. Ice concentration first dropped below 0.9 in mid-April, followed by a rapid decrease that started on May 10 and resulted in ice-free conditions by June 22.

[22] The observed annual $p\text{CO}_{2\text{sw}}$ cycle is displayed in Figure 2c. To briefly summarize the findings of *Else et al.* [2012a], $p\text{CO}_{2\text{sw}}$ was low ($\sim 300 \mu\text{atm}$) upon arrival in October 2007, likely due to SST cooling from a summer maximum and fall phytoplankton blooms. After ice formation, $p\text{CO}_{2\text{sw}}$ slowly increased due to brine rejection and associated convection, respiration, and gas exchange, reaching a maximum of $\sim 380 \mu\text{atm}$ in late March. This was followed by a gradual decrease in spring caused by an ice algae bloom, and then an accelerated decrease due to open water phytoplankton blooms that reduced $p\text{CO}_{2\text{sw}}$ to $\sim 300 \mu\text{atm}$ in early June. In mid-July $p\text{CO}_{2\text{sw}}$ increased rapidly to $\sim 410 \mu\text{atm}$ as a result of gas exchange and surface warming, and then began to decrease as the sea surface cooled.

[23] Atmospheric $p\text{CO}_2$ (Figure 2d) varied from $\sim 375 \mu\text{atm}$ in the fall to $\sim 395 \mu\text{atm}$ in mid-winter, following the expected global seasonal CO₂ pattern. These $p\text{CO}_{2\text{atm}}$ values kept $\Delta p\text{CO}_2$ negative for most of the annual cycle, except for a brief positive excursion in mid-July.

[24] Sea surface temperature through the study period is shown in Figure 2e. In the fall, SST reached the freezing point in mid-November, and then decreased slightly through the winter as the freezing point was lowered by increasing salinity (Figure 2f). A rapid increase in SST then started in mid-May as C_i decreased (Figure 2b), reaching a maximum near 8°C in mid-July. This was followed by a more gradual decrease in SST as waters cooled in the fall.

[25] Salinity followed a distinct cycle, which has been described thoroughly in *Shadwick et al.* [2011] (Figure 2f). At the beginning of the study period salinity was low (28–29), and then gradually increased to a maximum near 32 in April due largely to brine rejection by the growing ice cover and associated convection. As the ice began to melt in May, salinity decreased back towards fall values.

3.2. Calculated Fluxes

[26] The time series of calculated fluxes during the non-freezing season ($F_{\text{CO}_{2\text{as:norm}}}$) is shown in Figure 3. The strongest fluxes (up to $-40 \text{ mmol m}^{-2} \text{ d}^{-1}$) occurred in October 2007, when winds were highest (Figure 2a) and $\Delta p\text{CO}_2$ was strongly negative (Figures 2c & d). Significant CO₂ uptake by the ocean continued through most of November, but $F_{\text{CO}_{2\text{as:norm}}}$ was essentially cut off towards the end of the month when C_i began to consistently exceed 0.95 (Figure 2b). In early May, $F_{\text{CO}_{2\text{as:norm}}}$ resumed with small episodes of uptake, and then proceeded in earnest in late May and June as the ice cover was removed by wind forcing. Despite negative $\Delta p\text{CO}_2$ similar to the fall of 2007, maximum uptake rates during the spring were around $-30 \text{ mmol m}^{-2} \text{ d}^{-1}$ because of weaker winds. In July, a short period of outgassing (maximum $\sim 5 \text{ mmol m}^{-2} \text{ d}^{-1}$) occurred due to the mid-summer $p\text{CO}_{2\text{sw}}$ peak (Figure 2c). This was followed by modest uptake in August

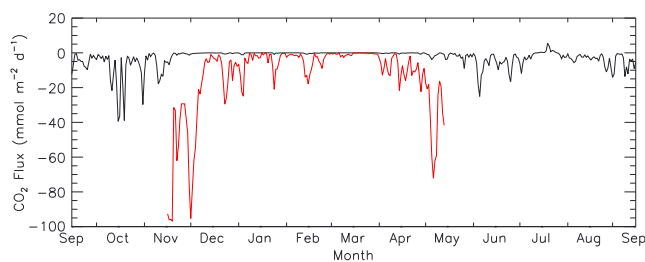


Figure 3. Calculated $F_{\text{CO}_{2\text{as:norm}}}$ (black line) and $F_{\text{CO}_{2\text{as:enh}}}$ (red line) for the study area.

and September (maximum $\sim -15 \text{ mmol m}^{-2} \text{ d}^{-1}$) due to the light wind conditions and moderately negative $\Delta p\text{CO}_2$. Overall, we calculated a mean $F_{\text{CO}_{2\text{as:norm}}}$ of $-5.2 \pm 2.0 \text{ mmol m}^{-2} \text{ d}^{-1}$ over the non-freezing period (184 days).

[27] Also shown in Figure 3 is our rough estimate of the winter enhanced flux ($F_{\text{CO}_{2\text{as:enh}}}$). These results show two key features: high-magnitude fluxes in the fall and spring, and weaker but still significant fluxes throughout the winter. The high flux estimates in the fall were a result of the large amounts of open water present as the ice began to form while $\Delta p\text{CO}_2$ was strongly negative (Figures 2b, c & d). This initial pulse of rapid uptake is consistent with the findings of *Anderson et al.* [2004], but to our knowledge the potential for strong uptake as polynyas form in the spring has not been previously identified. The high spring flux estimates occurred because under-ice primary production began to reduce $p\text{CO}_{2\text{sw}}$ in March and April [*Shadwick et al.*, 2011; *Else et al.*, 2012a] and when dynamic processes began to break up the ice in early May, the atmospheric conditions were still conducive to new ice formation and thus enhanced flux.

[28] The mean $F_{\text{CO}_{2\text{as:enh}}}$ calculated for the freezing period (182 days) was $-15.0 \pm 10.0 \text{ mmol m}^{-2} \text{ d}^{-1}$. If this estimate is reasonable, the amount of carbon transferred to the mixed layer by this exchange should be commensurate with dissolved inorganic carbon (DIC) budgets for the region. In the same study area, *Shadwick et al.* [2011] observed a mixed layer DIC increase over the 2007–08 winter period (which they defined as November 15 – March 15) of approximately $200 \mu\text{mol kg}^{-1}$. Assuming a 50 m mixed layer depth, the DIC increase resulting from $F_{\text{CO}_{2\text{as:enh}}}$ over that time period would be $\sim 37 \pm 30 \mu\text{mol kg}^{-1}$. *Shadwick et al.* [2011] constrained the winter increase in DIC due to brine rejection to be $\sim 97 \mu\text{mol kg}^{-1}$, and *Nguyen et al.* [2012] reported water column community respiration rates of $11.0 \pm 5 \mu\text{gC L}^{-1} \text{ d}^{-1}$ over the same time period, which would have increased DIC by $109 \pm 30 \mu\text{mol kg}^{-1}$. Summed up, these components (gas exchange, brine rejection, respiration) exceed the observed $200 \mu\text{mol kg}^{-1}$ DIC increase by 22%. However, we argue that the air–sea gas exchange rates can still be considered reasonable in light of this budget, given evidence that the respiration rates are likely overestimated [*Nguyen et al.*, 2012], and given the large uncertainties in the budget terms.

[29] Since the freezing period (184 days) is essentially equal in length to the non-freezing period (182 days), this estimated flux enhancement greatly increases the annual $F_{\text{CO}_{2\text{as}}}$ relative to simply computing $F_{\text{CO}_{2\text{as:norm}}}$ for the entire year. By combining the non-freezing and freezing season fluxes, we obtain a

total annual average F_{CO_2as} of $-10.1 \pm 6.5 \text{ mmol m}^{-2} \text{ d}^{-1}$ for the Cape Bathurst polynya region.

4. Discussion

4.1. How “Typical” Was 2007–08?

[30] Mean annual fluxes for a given region are often compiled in papers that attempt to budget air–sea gas exchange on larger scales (e.g. *Borges et al.* [2005]; *Cai et al.* [2006]; *Bates and Mathis* [2009]; *Chen & Borges* [2009]). This approach is most effective when the compiled studies provide some analysis of interannual variability. We do not have the data set necessary to calculate a complete annual budget for our study area over several years, but in this section we use other data sets to discuss the long–term variability in many of the parameters that directly affect CO₂ flux. The goal of this analysis is to determine if our mean annual flux estimate is typical of the mean state of the Cape Bathurst polynya, or if it represents a somewhat anomalous year.

4.1.1. pCO_{2sw} Conditions

[31] To examine interannual variability in pCO_{2sw} , we collected data from other cruises during which pCO_{2sw} measurements were carried out in the study region between 2003–2009. The first available data are from *Mucci et al.* [2010], who calculated pCO_{2sw} from surface DIC, pH, and total alkalinity (TA) measurements during fall 2003 and spring/summer 2004. In 2006, our research group made direct pCO_{2sw} measurements on the CCGS *Amundsen* using an underway instrument composed of a membrane contactor (Liqui-Cel SuperPhobic x50) and an LI-7000 gas analyzer, similar to a system described in *Else et al.* [2008a]. In 2009, we returned to the area, this time with a commercially built underway pCO_{2sw} system (General Oceanics model 8050), which has an expected accuracy of $2 \mu\text{atm}$ [*Pierrot et al.* 2009].

[32] The pCO_{2sw} measurements made during these cruises are shown in Figure 4 in comparison to the generalized cycle and variability observed in 2007–08. Despite the diversity in measurement techniques, there is remarkable consistency in pCO_{2sw} observations made between September and November, with most falling within ± 1 standard deviation of the 2007–08 measurements. This suggests that negative ΔpCO_2 and a decreasing trend in pCO_{2sw} as the sea surface cools is typical for the region in autumn, at least over the past decade.

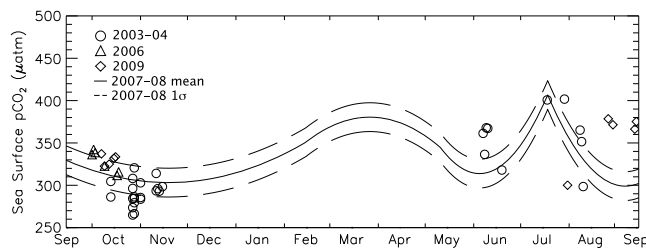


Figure 4. pCO_{2sw} observations made in the Cape Bathurst polynya region during other cruises in comparison to the polynomial fit of the 2007–08 pCO_{2sw} data. The dashed lines show \pm one standard deviation around the polynomial fit.

[33] The only other time period where we can make interannual comparisons is in the summer open water season. As Figure 4 shows, 2004 appeared to follow a similar pattern to 2008, with pCO_{2sw} increasing to a peak near $400 \mu\text{atm}$ in mid–July and then decreasing through August. It is worth noting that spring/summer ice cycles in 2004 followed a very similar pattern to 2008, with break–up occurring at essentially the same time. In 2009, pCO_{2sw} appeared to experience a similar summer pattern to 2008, but perhaps with a delayed increase (starting at the end of July) and a smaller peak value ($\sim 375 \mu\text{atm}$ in August). Ice break–up in 2009 occurred nearly one month later than in 2008, and the region did not become completely ice free until mid–August. This apparently delayed and reduced the summer pCO_{2sw} increase, possibly by limiting air–sea gas exchange and keeping SST low (SST reached a maximum of $\sim 5^\circ \text{ C}$ in 2009 compared to $\sim 8^\circ \text{ C}$ in 2008). These results suggests that variations in the annual pCO_{2sw} cycle may be linked to sea ice cycles, which raises the question of how typical the ice conditions were in 2007–08.

4.1.2. Ice Conditions

[34] We compared the 2007–08 ice conditions to a regional climatology based on the AMSR-E C_i data from 2002–2010 (Figure 5). In 2007, ice formation began about three weeks later than average, but reached a concentration of 0.80 only one week later than average. The winter leads and small polynyas generated by ice motion in 2007–08 are typical for the region, as evidenced by the long–term mean winter C_i below 1 and variability (standard deviation ~ 0.02) around that mean. The significant decline in C_i in mid–May 2008 was also typical, although the region became ice–free more than 4 weeks earlier than average. Overall, there were very few instances when C_i in 2007–08 fell outside of one standard deviation of the 2002–2010 mean. Therefore, the 2007–08 ice cycle could be described as a “light” ice year with late freeze–up and rapid spring break–up, but not anomalously light within the context of the last decade.

4.1.3. Wind Conditions

[35] Wind speed and direction in 2007–08 were grouped by season and compared to wind data collected at the Cape Parry weather station between 2000–2010. Figure 6 shows that fall 2007 wind velocities were significantly higher than average, but adhered to the usual easterly direction. Winter and spring 2007–08 winds also displayed a typically easterly direction with stronger than average velocities. Summer 2008 wind velocities were substantially higher than the long–term mean and were even more easterly than usual.

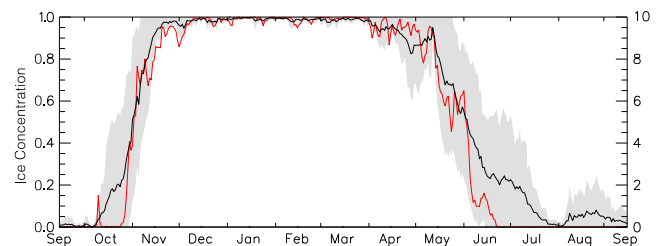


Figure 5. 2007–08 ice concentration in the Cape Bathurst polynya region (red line) compared to the 2002–10 mean (black line). The grey shaded area represents \pm one standard deviation around the 2002–10 mean.

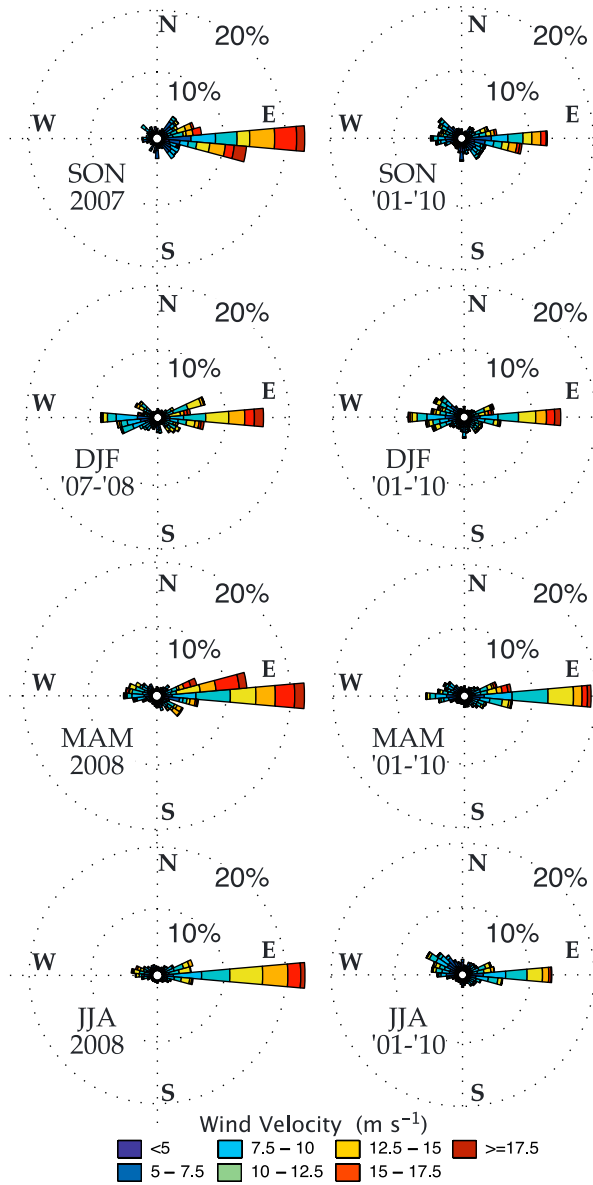


Figure 6. Wind rose plots comparing the frequency of hourly wind velocities and directions by season observed in 2007–08 (left column) to the 2001–10 mean (right column). SON=September, October, November; DJF=December, January, February; MAM=March, April, May; JJA=June, July, August. Data are from the Cape Parry Environment Canada weather station.

One-way analysis of variance (ANOVA) testing confirmed that mean wind velocities during all four seasons were significantly higher than the 2000–2010 seasonal averages. We can thus conclude that 2007–08 was an anomalously windy year, with winds predominantly from the east.

4.1.4. Sensitivity of the Computed Flux to Interannual Variability in Wind and Ice Conditions

[36] Although we cannot perform a complete analysis of interannual variability, we can examine the sensitivity of the mean annual $F_{\text{CO}_2\text{as}}$ to interannual variability in wind speed (U) and C_i . To do this, we held the 2007–08 $p\text{CO}_{2\text{sw}}$, SST, and salinity data constant, and then solved equation 2, applying the historical C_i and U data both independently and in

combination. The estimated enhanced gas transfer velocity was applied when C_i exceeded 0.80 in the fall and fell below 0.80 in the spring.

[37] As shown in Table 1, the calculated mean annual $F_{\text{CO}_2\text{as}}$ using this approach ranges from -6.0 to -12.4 $\text{mmol m}^{-2} \text{d}^{-1}$, with an average difference from 2007–08 of ± 1.7 $\text{mmol m}^{-2} \text{d}^{-1}$. Allowing only wind speed to vary showed a relatively weak impact on mean annual $F_{\text{CO}_2\text{as}}$ with a mean difference from 2007–08 of 0.6 $\text{mmol m}^{-2} \text{d}^{-1}$. However, the analysis shows a stronger sink (by 0.2 – 0.8 $\text{mmol m}^{-2} \text{d}^{-1}$) in 2007–08 than in any other year, suggesting that the abnormally strong winds enhanced CO₂ uptake in our study year. In contrast, by allowing only C_i to vary, $F_{\text{CO}_2\text{as}}$ ranges from a 3.3 $\text{mmol m}^{-2} \text{d}^{-1}$ stronger sink to a 2.9 $\text{mmol m}^{-2} \text{d}^{-1}$ weaker sink, indicating a high sensitivity to C_i . Much of this sensitivity arises from our estimate of $F_{\text{CO}_2\text{as}^{\text{enh}}}$, both in terms of the length of the season to which the estimate is applied (which ranges from 179–233 days), and the strength of the enhancement (which ranges from a mean of -7.6 – -21.2 $\text{mmol m}^{-2} \text{d}^{-1}$). Obviously, these numbers are somewhat speculative given the nature of our estimate of $F_{\text{CO}_2\text{as}^{\text{enh}}}$. Nevertheless, given the multiple influences that variability in C_i has on $F_{\text{CO}_2\text{as}}$ (including its potential role in contributing to variability in $p\text{CO}_{2\text{sw}}$), it is safe to say that the mean annual air–sea exchange of CO₂ in the Cape Bathurst polynya region is highly sensitive to C_i .

4.2. Large Scale Atmosphere/Ocean Circulation and CO₂ Fluxes in the Cape Bathurst Polynya

[38] Given the critical role of sea ice, it is interesting to consider the two remarkable events that bookended the 2007–08 year: the record low Arctic sea ice extent in September 2007 (since eclipsed by the September 2012 minimum), and the second–lowest recorded sea ice extent in September 2008. Those events raise the question of whether some of the conditions we observed in the Cape Bathurst polynya were influenced by the same factors that drove hemispheric–scale reductions in sea ice extent.

[39] In Figure 7, we show the seasonal sea level pressure in the Arctic during 2007–08, which reveals high pressure on the North American side of the Arctic for most of the year. Intense high–pressure was particularly obvious over the Beaufort Sea in fall 2007 and spring 2008. A strong Beaufort high drives anti–cyclonic circulation, explaining the strong easterly winds that we experienced during these seasons (Figures 2, 6). It also may explain some of the ice conditions we experienced, in particular the late fall freeze–up and the early spring break–up.

[40] Galley *et al.* [2009] hypothesized that the spring opening of the Cape Bathurst polynya is largely driven by easterly winds. We investigated this hypothesis using the ice–out dates between 1980–2004 reported by Galley *et al.* [2008], and found that easterly winds in March–April–May are indeed significantly correlated ($p < 0.01$) with earlier polynya opening dates ($r = 0.59$). It seems likely, therefore, that the early ice free conditions experienced in the spring of 2008 were driven to some extent by winds associated with the high pressure anomaly in the Beaufort Sea.

[41] Although easterly winds in June–July–August are likewise significantly correlated ($r = -0.50$, $p < 0.01$) with later freeze–up dates, the relationship between freeze–up date and large scale pressure variability is more complex. One

Table 1. Estimated Impacts of Interannual Variability in Sea Ice Concentration and Wind Speed on Air-Sea CO₂ Flux

Year	Wind Velocity (m s ⁻¹)				Ice Concentration				Mean F_{CO_2as} Both Vary	F_{CO_2as} vs '07-'08 Ice Vary	F_{CO_2as} vs '07-'08 Wind Vary
	SON mean (std dev)	DJF mean (std dev)	MAM mean (std dev)	JJA mean (std dev)	Freeze Up Date	Break Up Date	Winter C_i mean (stddev)	Mean $F_{CO_2as,enh}$ Both Vary			
2000-01	5.2 (2.9)	5.6 (3.7)	5.2 (2.8)	4.6 (2.8)	-	-	-	-	-	0.8	
2001-02	5.6 (3.7)	5.1 (3.4)	4.9 (3.1)	4.3 (2.6)	-	-	-	-	-	0.8	
2002-03	6.1 (3.9)	5.2 (3.3)	4.5 (3.3)	3.9 (2.6)	15-Oct	17-Apr	0.962 (0.064)	-21.2	-3.2	0.6	
2003-04	5.6 (3.5)	6.1 (3.6)	5.7 (3.8)	4.2 (3.1)	1-Nov	25-May	0.980 (0.038)	-6.0	2.9	0.7	
2004-05	5.2 (3.6)	6.4 (3.8)	6.0 (3.7)	4.6 (2.8)	26-Oct	10-May	0.957 (0.060)	-14.0	-0.3	0.6	
2005-06	6.4 (3.7)	6.1 (3.6)	5.1 (2.9)	4.4 (2.4)	2-Nov	23-Jun	0.974 (0.041)	-8.9	0.2	0.5	
2006-07	5.9 (3.5)	6.0 (3.8)	5.4 (3.4)	4.1 (2.5)	12-Nov	4-Jun	0.970 (0.044)	-13.4	-0.5	0.7	
2007-08	6.9 (4.6)	6.4 (3.6)	6.6 (3.9)	5.8 (3.2)	16-Nov	13-May	0.967 (0.043)	-15.0	-	-	
2008-09	5.5 (3.2)	5.5 (2.8)	5.1 (2.7)	5.1 (3.1)	8-Nov	10-Jun	0.961 (0.060)	-18.1	-3.3	0.4	
2009-10	6.1 (3.9)	5.8 (3.3)	6.1 (3.5)	5.4 (2.8)	9-Nov	17-May	0.973 (0.032)	-10.8	1.4	0.2	

Columns 2-5 give seasonal (SON = September, October, November, DJF = December, January, February, MAM = March, April, May, JJA = June, July, August) mean/standard deviation wind velocities for each year. Columns 6-8 present sea ice concentration data for each year. Columns 9-10 show the total (including the enhanced fluxes) and winter CO₂ flux (respectively). Columns 11-12 show the difference in total flux relative to 2007-08 if only ice concentration or wind speed is allowed to vary.

important control which may drive earlier freeze-up in Amundsen Gulf is the intrusion of an “ice tongue” from the Beaufort pack ice. *Galley et al.* [2008] show that this ice tongue existed in about 40% of years between 1980–2004, and *Galley et al.* [2009] proposed that its presence seeds ice formation in Amundsen Gulf, potentially leading to earlier freeze-up. A strong Beaufort high (such as we observed in fall 2007) drives anticyclonic ice motion in the Beaufort Gyre, which moves ice away from the archipelago [*Kwok, 2006; Lukovich and Barber, 2006*], likely inhibiting the intrusion of this ice tongue. Certainly, archived data from the Canadian Ice Service show there was no ice tongue present in Amundsen Gulf in fall 2007, which may account for the late freeze-up.

[42] Based on this discussion, the timing of open water in the Cape Bathurst polynya was likely linked to pressure patterns in the Beaufort Sea, both through controls on wind forcing in Amundsen Gulf, and through behaviour of sea ice in the Beaufort Gyre. One of the major causes of the anomalous basin-wide conditions in 2007 and 2008 was the persistence of a strong “Dipole Anomaly” (DA), a statistical description of sea level pressure variability in the Arctic [*Wang et al., 2009; Overland and Wang, 2010b*]. The phase of the DA that persisted for all of 2007 and 2008 is associated with anomalously high pressure on the North American side of the Arctic [*Wang et al., 2009*], as is apparent in Figure 7. Given the important role that this pressure pattern played in influencing our observations in 2007–08, the DA may be useful in explaining conditions in the Cape Bathurst polynya.

[43] If this hypothesis of a link between strong easterly winds, light ice conditions, and a dominant DA is sound, our presence in the Cape Bathurst polynya in 2007–08 was particularly fortuitous. The Arctic Ocean appears to have transitioned from a period where the positive phase of the Arctic Oscillation dominates circulation patterns, to one in which the DA is dominant [*Overland and Wang, 2010a; Maslanik et al., 2007*]. Therefore, the 2007–08 CO₂ flux budget that we have calculated for the Cape Bathurst polynya may be representative of the region under contemporary circulation patterns. Although the emergence of the DA is difficult to explain (and thus difficult to predict), it may in part be due to climate warming as a result of anthropogenic forcings [*Zhang et al., 2008*]. If the pattern were to intensify as those forcings intensify, we might expect higher easterly winds, earlier break-up, later freeze-up, and more winter ice motion in the Cape Bathurst polynya, all of which would increase atmospheric CO₂ uptake.

4.3. Implications at the Circumpolar Scale

[44] Our study area is an example of the many coastal polynyas distributed around the circumpolar Arctic (e.g. *Barber and Massom [2007]*). If the rates of atmospheric CO₂ uptake that we estimated are similar in other Arctic polynyas, then the Arctic-wide uptake of CO₂ through these features may be significant. Of particular interest is the winter CO₂ uptake. In the Storfjorden polynya, *Omar et al.* [2005] estimated a mean winter CO₂ flux of -14.8 mmol m⁻² d⁻¹, and performed a simple extrapolation to calculate a total winter uptake for all Arctic coastal polynyas of 2.3×10^{12} gC yr⁻¹. This uptake rate is on the same order of magnitude as that observed in many mid- and high-latitude shelf seas [*Cai et al., 2006*], despite the total area of coastal polynyas being relatively small. The

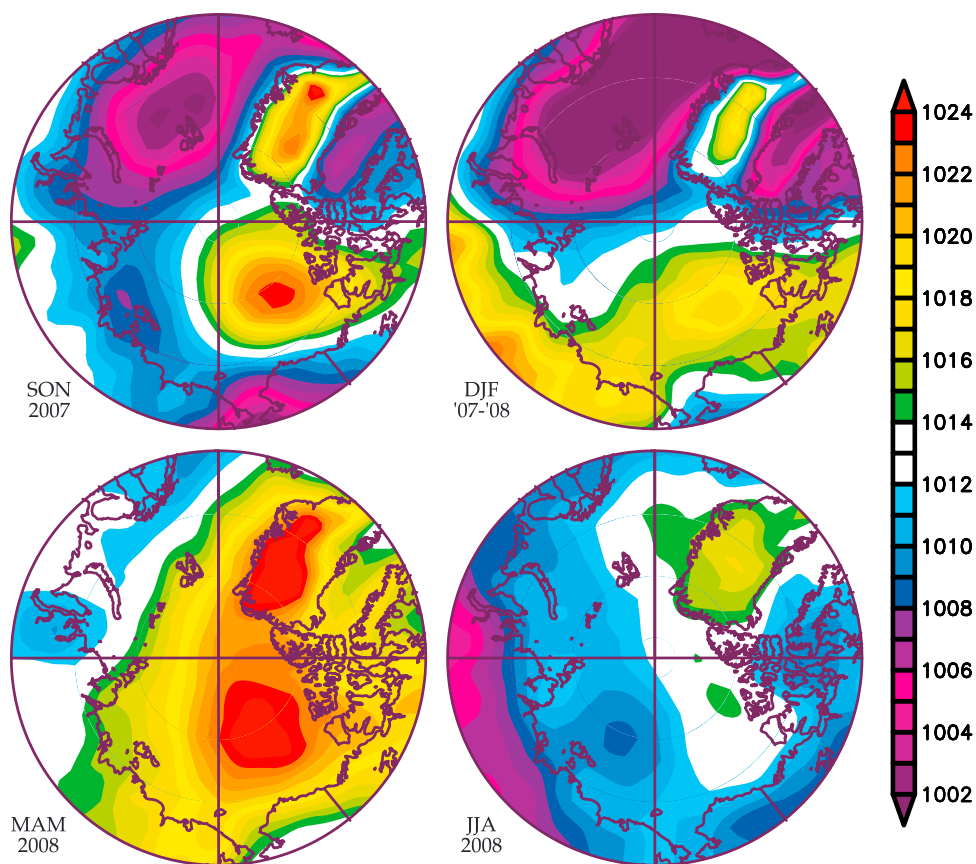


Figure 7. Mean seasonal sea level pressure (in mbar) for the Arctic in 2007–08. SON=September, October, November; DJF=December, January, February; MAM=March, April, May; JJA=June, July, August. Data are from the NCEP/NAR reanalysis (Kalnay, 1996), plotted using the web-based plotting tools of the NOAA/ESRL Physical Sciences Division (Boulder, Colorado).

finding is particularly significant, because at least some of the carbon absorbed by this processes is expected to be removed from further exchange with the atmosphere via the formation of deep and intermediate water by brine rejection [Omar *et al.*, 2005].

[45] Our estimated rate of winter uptake for the Cape Bathurst polynya region ($-15.1 \pm 10.0 \text{ mmol m}^{-2} \text{ d}^{-1}$) is remarkably similar to the rates found by [Omar *et al.* [2005], lending support to their theory that polynyas play a significant role in CO₂ sequestration. If we extrapolate our mean winter flux to the same area that Omar *et al.* [2005] used for coastal polynyas ($3.5 \times 10^{10} \text{ m}^2$) and assume a 184-day freezing season (section 3.2), we calculate a slightly smaller uptake for Arctic coastal polynyas of $1.2 \times 10^{12} \text{ gC yr}^{-1}$. Even the lower rate of exchange that we estimated can be partly explained by differences between the two regions; the Storfjorden polynya opens periodically through the winter, keeping the mean open water fraction relatively high (7–13%, Skogseth *et al.* [2005]), while the Cape Bathurst polynya does not experience a large-scale opening until spring, with a lower open water fraction in winter (2–4%, Table 1). This illustrates that upscaling will result in an estimate biased by the peculiarities of the model polynya, but our results support Omar *et al.* [2005]’s conclusion that their estimate is of the right order of magnitude.

[46] We caution, however, that further investigations are required to confirm if negative $\Delta p\text{CO}_2$ throughout the

winter is a typical state for Arctic polynya regions. Along the southern margins of Amundsen Gulf and on the Mackenzie Shelf, we observed episodes of strongly positive $\Delta p\text{CO}_2$ associated with wind-driven upwelling events in the late fall [Else *et al.*, 2012a, 2012b]. We do not know if that upwelling persisted through the winter, but it is quite plausible that certain polynyas may be sustained by upwelling-favourable winds, or that ice motion in a polynya may drive winter upwelling (e.g. McPhee *et al.* [2005]). Furthermore, evidence of winter supersaturation has been presented for the Northwater polynya [Miller *et al.*, 2002] and in landfast ice near the re-occurring flaw lead north of Point Barrow, Alaska [Semiletov *et al.*, 2007]. If polynya or flaw lead regions with supersaturated winter $p\text{CO}_{2,\text{sw}}$ are in fact widespread, then the CO₂ uptake estimate of Omar *et al.* [2005] must be offset to some degree by such regions.

[47] During the non-freezing seasons, Arctic shelf seas typically absorb CO₂ at rates between -1.0 to $-15 \text{ mmol m}^{-2} \text{ d}^{-1}$ (see for example Table 3 in Else *et al.* [2008b]). The mean CO₂ uptake rate that we observed ($-5.2 \pm 2.0 \text{ mmol m}^{-2} \text{ d}^{-1}$) is median to that range, although considerable variability in both the magnitude and direction occurred over the ice-free season (Figure 3). Our results thus reinforce the paradigm that, with a few notable exceptions (e.g. Anderson *et al.* [2009]), Arctic shelf seas generally absorb atmospheric CO₂ during non-freezing seasons [Bates and Mathis, 2009].

5. Summary and Conclusions

[48] The potential role of polynya regions as atmospheric CO₂ sinks has long been acknowledged [Yager *et al.*, 1995], but opportunities for thorough investigation have been rare. This study shows that the Cape Bathurst polynya region does indeed act as a strong CO₂ sink, but not entirely for the reasons that Yager *et al.* [1995] suggested. Yager *et al.* [1995] hypothesized that in spring-opening polynya regions, potential winter outgassing would be prevented by a sea ice cover. In contrast, we found that in the presences of a broken and mobile ice cover, a persistently negative $\Delta p\text{CO}_2$ coupled with an enhanced rate of gas exchange allowed CO₂ uptake through the winter at a mean rate in excess of the open water seasons. When combined with the exchange that occurred through the other seasons, our calculated mean annual rate of CO₂ uptake for this region was approximately 3 times higher than the preliminary estimate of Shadwick *et al.* [2011].

[49] A sensitivity analysis on the effect of variability in wind and ice conditions on CO₂ exchange revealed that anomalously strong winds during 2007–08 likely enhanced CO₂ uptake relative to the decadal mean. Further adding to the strong uptake were light ice conditions, characterized by a late freeze-up (by ~ 3 weeks) and early breakup (by ~ 4 weeks). The light ice conditions may have been caused in part by the strong easterly winds, and in turn appeared to influence the $p\text{CO}_{2,\text{sw}}$ cycle. Both the wind and ice conditions that we observed in 2007–08 were likely controlled by a strong north–south pressure gradient, a characteristic of the Arctic Dipole phase that was particularly strong through the study period. If that phase of the Arctic Dipole pattern becomes the norm for the Arctic (as recent observations by Overland and Wang [2005] and Maslanik *et al.* [2007] suggest), then the mean annual CO₂ flux we estimated for 2007–08 may be quite representative of current and future air–sea CO₂ exchange in the region.

[50] Net annual uptake of atmospheric CO₂ by the Cape Bathurst polynya region agrees with the paradigm that most Arctic shelf seas act as sinks for atmospheric CO₂. Bates and Mathis [2009] estimated that the Arctic Ocean absorbs $0.6\text{--}1.9 \times 10^{14}$ gC yr⁻¹ during the open water seasons, and our estimated open water CO₂ fluxes are within the range of observations used to arrive at that conclusion. More interestingly, our study also supports an emerging school of thought that the Arctic Ocean may absorb a significant amount of CO₂ during the winter. Although initial order-of-magnitude estimates indicate that the total winter flux is smaller than the open water flux (10^{12} gC yr⁻¹ vs. 10^{14} gC yr⁻¹), the area through which this exchange occurs is smaller by a similar magnitude. Thus, if the area of winter open water increases, absorption of CO₂ via this pathway could become more significant. The potential for increased winter open water is a distinct possibility, given the recent decline of multi-year ice [Maslanik *et al.*, 2011], drastic decreases in summer sea ice extent (e.g. Stroeve *et al.* [2007]), and observations of increased winter ice motion [Hakkinen *et al.*, 2008]. However, testing of this hypothesis requires a better understanding and quantification of the flux enhancements that occur in winter open water features, and an extensive survey of winter $\Delta p\text{CO}_2$ throughout the Arctic.

[51] **Acknowledgments.** Thanks to the Captains and crew of the CCGS *Amundsen* and the many people who helped in the field: Bruce Johnson, Sarah Woods, Kyle Swystun, Gauthier Camat, Nes Sutherland,

Keith Johnson, Jens Ehn, Silvia Gremes-Cordero, Sylvain Blondeau, Luc Michaud and many others. CTD data were provided by Yves Gratton. This work is a contribution to the International Polar Year-Circumpolar Flaw Lead system study (IPY-CFL 2008), supported by the Canadian IPY Federal program office, the Natural Sciences and Engineering Research Council (NSERC), and many other contributors. The authors of this paper are members of ArcticNet, funded in part by the Networks of Centres of Excellence (NCE) Canada, NSERC, the Canadian Institute of Health Research and the Social Sciences and Humanities Research Council. B. Else is supported by a Vanier Canada Graduate Scholarship, and received funding for logistics from the Northern Scientific Training Program. We gratefully acknowledge the continued support of the Centre for Earth Observation Science, the Canada Excellence Research Chair (CERC) in Arctic Geomicrobiology and Climate Change, and the University of Manitoba.

References

- Anderson, L. G., E. Falck, E. P. Jones, S. Jutterström, and J. H. Swift (2004), Enhanced uptake of atmospheric CO₂ during freezing of seawater: A field study in Storfjorden, Svalbard. *J. Geophys. Res.*, *109*, C06004, doi:10.1029/2003JC002120.
- Anderson, L. G., S. Jutterström, S. Hjalmarsson, I. Wählström, and I. P. Semiletov (2009), Out-gassing of CO₂ from Siberian Shelf seas by terrestrial organic matter decomposition. *Geophys. Res. Lett.*, *36*, L20601, doi:10.1029/2009GL040046.
- ArcticNet (2010), Impacts of environmental change in the Canadian Coastal Arctic: A compendium of research conducted during ArcticNet Phase I (2004–2008). ArcticNet Inc., Québec City, Canada.
- Barber, D. G. and R. A. Massom (2007), The role of sea ice in Arctic and Antarctic polynyas. In *Polynyas: Windows to the World*, edited by W. O. Smith, Jr. and Barber D. G., volume 74 of Elsevier Oceanography Series, chapter 1, pages 1–54, Elsevier.
- Barber, D. G., M. G. Asplin, Y. Gratton, J. V. Lukovich, R. J. Galley, R. L. Raddatz and D. Leitch (2010), The International Polar Year (IPY) Circumpolar Flaw Lead (CFL) System Study: Overview and the Physical System. *Atmosphere-Ocean*, *48*, 225–243, doi:10.3137/OC317.2010
- Bates, N. R., and J. T. Mathis (2009), The Arctic Ocean marine carbon cycle: evaluation of air–sea CO₂ exchanges, ocean acidification impacts and potential feedbacks. *Biogeosciences*, *6*(11):2433–2459.
- Borges, A. V., B. Delille, and M. Frankignoulle (2005), Budgeting sinks and sources of CO₂ in the coastal ocean: Diversity of ecosystems counts. *Geophys. Res. Lett.*, *32*, L14601, doi:10.1029/2005GL023053.
- Cai, W. -J., M. Dai, and Y. Wang (2006), Air–sea exchange of carbon dioxide in ocean margins: A province-based synthesis. *Geophys. Res. Lett.*, *33*, L12603, doi:10.1029/2006GL026219.
- Chen, C.-T. A., and A. V. Borges (2009), Reconciling opposing views on carbon cycling in the coastal ocean: Continental shelves as sinks and near-shore ecosystems as sources of atmospheric CO₂. *Deep-Sea Research II*, *56*, 578–590.
- Else, B. G. T., T. Papakyriakou, M. Granskog, and J. Yackel (2008a), Observations of sea surface $f\text{CO}_2$ distributions and estimated air–sea CO₂ fluxes in the Hudson Bay region (Canada) during the open water season. *J. Geophys. Res.*, *113*, C08026, doi:10.1029/2007JC004389.
- Else, B. G. T., J. J. Yackel and T. N. Papakyriakou (2008b), Application of satellite remote sensing techniques for estimating air–sea CO₂ fluxes in Hudson Bay, Canada during the ice-free season. *Remote Sens. Environ.*, *112*, 3550–3562, doi:10.1029/2007JC004389.
- Else, B. G. T., T. N. Papakyriakou, R. J. Galley, W. M. Drennan, L. A. Miller, and H. Thomas (2011), Wintertime CO₂ fluxes in an Arctic polynya using eddy covariance: Evidence for enhanced air–sea gas transfer during ice formation. *J. Geophys. Res.*, *116*, C00G03, doi:10.1029/2010JC006760.
- Else, B. G. T., T. N. Papakyriakou, A. Galley Mucci, M. Gosselin, L. A. Miller, E. H. Shadwick, and H. Thomas (2012a), Annual cycles of $p\text{CO}_{2,\text{sw}}$ in the southeastern Beaufort Sea: New understandings of air–sea CO₂ exchange in Arctic polynyas. *J. Geophys. Res.*, *117*, C00G13, doi:10.1029/2011JC007346.
- Else, B. G. T., R. J. Galley, T. N. Papakyriakou, L. A. Miller, A. Mucci, and D. Barber (2012b), Sea surface $p\text{CO}_2$ cycles and CO₂ fluxes at landfast sea ice edges in Amundsen Gulf, Canada. *J. Geophys. Res.*, *117*, C09010, doi:10.1029/2012JC007901.
- Galley, R. J., E. Key, D. G. Barber, B. J. Hwang, and J. K. Ehn (2008), Spatial and temporal variability of sea ice in the southern Beaufort Sea and Amundsen Gulf: 1980–2004. *J. Geophys. Res.*, *113*, C05S95, doi:10.1029/2007JC004553.
- Galley, R. J., D. G. Barber, E. Key, and S. Prinsenberg (2009), A physical explanation of the formation of the Cape Bathurst polynya, NWT, Canada. In *Sea ice thermodynamic and dynamic processes in the ocean–sea ice–atmosphere system of the Canadian Arctic*, pages 205–240, University of Manitoba PhD Thesis.

- Geilfus, N.-X., G. Carnat, T. Papakyriakou, J.-L. Tison, B. Else, H. Thomas, E. Shadwick, and B. Delille (2012), Dynamics of pCO₂ and related air–ice CO₂ fluxes in the Arctic coastal zone (Amundsen Gulf, Beaufort Sea). *J. Geophys. Res.*, *117*, C00G10, doi:10.1029/2011JC007118.
- Hakkinen S., A. Proshutinsky, and I. Ashik (2008). Sea ice drift in the Arctic since the 1950s. *Geophys. Res. Lett.*, *35*, L19704, doi:10.1029/2008GL034791.
- Kalnay, E. and co-authors (1996), The NCEP/NCAR reanalysis 40-year project. *Bull. Amer. Meteor. Soc.*, *77*, 437–471
- Keeling, C.D., S.C. Piper, R.B. Bacastow, M. Wahlen, T.P. Whorf, M. Heimann, and H. A. Meijer (2001), Exchanges of atmospheric CO₂ and ¹³CO₂ with the terrestrial biosphere and oceans from 1978 to 2000. I. Global Aspects, SIO Reference Series, No. 01-06, Scripps Institution of Oceanography, San Diego, p 88.
- Kwok, R. (2006). Exchange of sea ice between the Arctic Ocean and the Canadian Arctic Archipelago. *Geophys. Res. Lett.*, *33*, L16501, doi:10.1029/2006GL027094.
- Loose, B., W. R. McGillis, P. Schlosser, D. Perovich, and T. Takahashi (2009), Effects of freezing, growth, and ice cover on gas transport processes in laboratory seawater experiments. *Geophys. Res. Lett.*, *36*, L05603, doi:10.1029/2008GL036318.
- Loose, B., and W. R. Schlosser (2011), Sea ice and its effect on CO₂ flux between the atmosphere and the Southern Ocean interior. *J. Geophys. Res.*, *116*, doi:10.1029/2010JC006509.
- Lukovich, J. V., and D. G. Barber (2006), Atmospheric controls on sea ice motion in the southern Beaufort Sea. *J. Geophys. Res.*, *111*, D18103, doi:10.1029/2005JD006408.
- Maslanik, J., B. Drobot, C. Fowler, W. Emery, and R. Barry (2007), On the Arctic climate paradox and the continuing role of atmospheric circulation in affecting sea ice conditions. *Geophys. Res. Lett.*, *34*, L03711, doi:10.1029/2006GL028269.
- Maslanik, J., J. Stroeve, C. Fowler, and W. Emery (2011), Distribution and trends in Arctic sea ice age through spring 2011. *Geophys. Res. Lett.*, *38*, L13502, doi:10.1029/2011GL047735.
- Masson, D., and LeBlond P.H. (1989). Spectral evolution of wind-generated surface gravity waves in a dispersed ice field. *J. Fluid Mech.*, *202*, 43–81.
- McGillis, W. R., et al. (2004). Air–sea CO₂ exchange in the equatorial Pacific. *J. Geophys. Res.*, *109*:C08S02, doi:10.1029/2003JC002256.
- McPhee, M. G., (2005). Turbulent heat flux in the upper ocean under sea ice. *J. Geophys. Res.*, *97*, 5365–5379, doi:10.1029/92JC00239.
- McPhee, M. G., R. Kwok, R. Robins, and M. Coon (2005), Upwelling of Arctic pycnocline associated with shear motion of sea ice. *Geophys. Res. Lett.*, *32*, L10616, doi:10.1029/2004GL021819.
- Miller L.A., et al. (2002). Carbon distributions and fluxes in the North Water, 1998 and 1999. *Deep-Sea Research II*, *49*:5151–5170, doi:10.1016/S0967-0645(02)00183-2.
- Miller, L. A. and G. R. DiTullio (2007), Gas fluxes and dynamics in polynyas. In *Polynyas: Windows to the World*, edited by W. O. Smith, Jr. and Barber D.G., volume 74 of Elsevier Oceanography Series, chapter 5, pages 163–191, Elsevier.
- Miller, L. A., T. N. Papakyriakou, R. E. Collins, J. W. Deming, J. K. Ehn, R. W., Macdonald, A. Mucci, O. Owens, M. Raudsepp, and N. Sutherland (2011), Carbon dynamics in sea ice: A winter flux time series. *J. Geophys. Res.*, *116*, C02028, doi:10.1029/2009JC006058.
- Mucci, A., B. Lansard, L. A. Miller, and T. N. Papakyriakou (2010), CO₂ fluxes across the air–sea interface in the southeastern Beaufort Sea: Ice-free period. *J. Geophys. Res.*, *115*, C04003, doi:10.1029/2009JC005330.
- Nguyen, D., R. Maranger, J.-É. Tremblay, and M. Gosselin (2012). Respiration and bacterial carbon dynamics in the Amundsen Gulf, western Canadian Arctic. *J. Geophys. Res.*, *117*:C00G16, doi:10.1029/2011JC007343.
- Nomura, D., H. Yoshikawa-Inoue, and T. Toyota (2006). The effect of sea-ice growth on air–sea CO₂ flux in a tank experiment. *Tellus B*, *58*, 418–426, doi:10.1111/j.1600-0889.2006.00204.x.
- Nomura, D., H. Eicken, R. Gradinger, and K. Shirasawa. (2010), Rapid physically driven inversion of the air–sea ice CO₂ flux in the seasonal landfast ice off Barrow, Alaska after onset of surface melt. *Cont. Shelf Res.*, *36*, L17601, doi:10.1016/j.csr.2010.09.014.
- Omar, A., T. Johannessen, R. G. J. Bellergy, A. Olsen, L. G. Anderson, and Kivimäe (2005). Sea–ice and brine formation in Storfjorden: Implications for the Arctic wintertime air–sea CO₂ flux. In *The Nordic Seas: an Integrated Perspective*, edited by H. Drange T. Dokken T. Furevik R. Gerdes W. Berger, American Geophysical Union, Geophysical Monograph 158, 177–189.
- Overland, J. E., and M. Wang (2010a). The Arctic climate paradox: The recent decrease of the Arctic Oscillation. *Geophys. Res. Lett.*, *32*, L06701, doi:10.1029/2004GL021752.
- Overland, J. E., and M. Wang (2010b), Large-scale atmospheric circulation changes are associated with the recent loss of Arctic sea ice. *Tellus*, *62A*, 1–9, doi:10.1111/j.1600-0870.2009.00421.x.
- Papakyriakou, T. and L. Miller (2011), Springtime CO₂ exchange over seasonal sea ice in the Canadian Arctic Archipelago, *Annals of Glaciology*, *52*, 215–224.
- Pierrot, D., C. Neill, K. Sullivan, R. Castle, R. Wanninkhof, H. Lüger, T. Johannessen, A. Olsen, R.A. Feeley and C. E. Cosca (2009), Recommendations for autonomous underway pCO₂ measuring systems and data–reduction routines. *Deep-Sea Research II*, *56*, 512–522, doi:10.1016/j.dsr2.2008.12.005.
- Semiletov, I., A. Makshtas, S.-I. Akasofu, and E. L. Andreas (2004), Atmospheric CO₂ balance: the role of Arctic sea ice. *Geophys. Res. Lett.*, *31*, L05121, doi:10.1029/2003GL017996.
- Semiletov, I. P., I. I. Pipko, I. Repina, and N. E. Shakhova (2007), Carbonate chemistry dynamics and carbon dioxide fluxes across the atmosphere–ice–water interfaces in the Arctic Ocean: Pacific sector of the Arctic. *J. Mar. Syst.*, *66*, 204–226, doi:10.1016/j.jmarsys.2006.05.012.
- Skogseth, R., I. Fer and Haugen P. M. (2005), Dense-water production and overflow from an Arctic coastal polynya in Storfjorden. In *The Nordic Seas: an Integrated Perspective*, edited by H. Drange T. Dokken T. Furevik R. Gerdes W. Berger, American Geophysical Union, Geophysical Monograph 158, 73–88.
- Shadwick, E. H., et al. (2011), Seasonal variability of the inorganic carbon system in the Amundsen Gulf region of the southeastern Beaufort Sea. *Limnol. Oceanogr.*, *56*, 303–322, doi:10.4319/lo.2011.56.1.0303.
- Spreen, G., L. Kaleschke, and G. Heygster (2008), Sea ice remote sensing using AMSR–E 89–GHz channels. *J. Geophys. Res.*, *113*, C02S03, doi:10.1029/2005JC003384.
- Stroeve, J., M. M. Holland, W. Meier, T. Scambos, and M. Serreze (2007), Arctic sea ice decline: Faster than forecast. *Geophys. Res. Lett.*, *34*, L09501, doi:10.1029/2007GL029703.
- Sweeney, C. (2003), The annual cycle of surface water CO₂ and O₂ in the Ross Sea: A model for gas exchange on the continental shelves of Antarctica. In *Biogeochemistry of the Ross Sea*, vol. 78 of Antarctic Research Series, edited by G. DiTullio, and R. Dunbar, pp. 295–312, American Geophysical Union, Washington, D.C.
- Sweeney, C., E. Gloor, A. R. Jacobson, R. M. Key, G. McKinley, J. L. Sarmiento, and R. Wanninkhof (2007), Constraining global air–sea gas exchange for CO₂ with recent bomb ¹⁴C measurements. *Global Biogeochem. Cycles*, *21*, GB2015, doi:10.1029/2006GB002784.
- Sweeney, C., D. A. Hansell, C. A. Carlson, L. A. Codispoti, L. I. Gordon, J. Marra, F.J. Millero, W.O. Smith and T. Takahashi (2000), Biogeochemical regimes, net community production and carbon export in the Ross Sea, Antarctica. *Deep-Sea Research II*, *47*, pp 3369–3394, doi:10.1016/S0967-0645(00)00072-2.
- Takahashi, T., J. Olafsson, J. G. Goddard, D. W. Chipman, and S. C. Sutherland (1993), Seasonal variation of CO₂ and nutrients in the high-latitude surface oceans: a comparative study. *Global Biogeochem. Cycles*, *7*(4), 843–878.
- Vickers, D. and L. Mahrt (1997), Fetch limited drag coefficients. *Boundary Layer Meteorol.*, *85*, 53–79.
- Wang, J., J. Zhang, E. Watanabe, M. Ikeda, K. Mizobata, J.E. Walsh, X. Bai, and B. Wu (2009), Is the Dipole Anomaly a major driver to record lows in Arctic summer sea ice extent?. *Geophys. Res. Lett.*, *36*, L05706, doi:10.1029/2008GL036706.
- Winsor, P. and G. Bjørk (2000), Polynya activity in the Arctic Ocean from 1958 to 1997. *J. Geophys. Res.*, *105*(C4), 8789–8803, doi:10.1029/1999JC900305.
- Woolf, D. K. (2005), Parameterization of gas transfer velocities and sea–state–dependent wave breaking. *Tellus*, *57B*, 87–94, doi:10.1111/j.1600-0889.2005.00139.x.
- Yager, P. L., D. W. R. Wallace, K. M. Johnson, Jr. W. O. Smith, P. J. Minnett, and J. W. Deming (1995), The Northeast Water Polynya as an atmospheric CO₂ sink: A seasonal rectification hypothesis. *J. Geophys. Res.*, *100*(C3), 4389–4398, doi:10.1029/94JC01962.
- Zappa, C. J., W. E. Asher, A. T. Jessup, J. Klinck and S. R. Long (2004), Microbreaking and the enhancement of air–water transfer velocity. *J. Geophys. Res.*, *106*, C08S16, doi:10.1029/2003JC001897.
- Zemmelink, H. J., B. Delille, J. L. Tison, E. Hintsala, L. Houghton, and J. J. Dacey, (2006), CO₂ deposition over the multi-year ice of the western Weddell Sea. *Geophys. Res. Lett.*, *33*, L13606, doi:10.1029/2006GL026320.
- Zhang, X., and A. Sorteberg, and J. Zhang, and R. Gerdes, and J. C. Comiso (2008), Recent radical shifts of atmospheric circulations and rapid changes in Arctic climate system. *Geophys. Res. Lett.*, *35*, L22701, doi:10.1029/2008GL035607.